doi:10.1038/nature13957

Direct human influence on atmospheric CO_2 seasonality from increased cropland productivity

Josh M. Gray[1], Steve Frolking[2], Eric A. Kort[3], Deepak K. Ray[4], Christopher J. Kucharik[5], Navin Ramankutty[6]† & Mark A. Friedl[1]

Ground- and aircraft-based measurements show that the seasonal amplitude of Northern Hemisphere atmospheric carbon dioxide (CO_2) concentrations has increased by as much as 50 per cent over the past 50 years[1–3]. This increase has been linked to changes in temperate, boreal and arctic ecosystem properties and processes such as enhanced photosynthesis, increased heterotrophic respiration, and expansion of woody vegetation[4–6]. However, the precise causal mechanisms behind the observed changes in atmospheric CO_2 seasonality remain unclear[2–4]. Here we use production statistics and a carbon accounting model to show that increases in agricultural productivity, which have been largely overlooked in previous investigations, explain as much as a quarter of the observed changes in atmospheric CO_2 seasonality. Specifically, Northern Hemisphere extratropical maize, wheat, rice, and soybean production grew by 240 per cent between 1961 and 2008, thereby increasing the amount of net carbon uptake by croplands during the Northern Hemisphere growing season by 0.33 petagrams. Maize alone accounts for two-thirds of this change, owing mostly to agricultural intensification within concentrated production zones in the midwestern United States and northern China. Maize, wheat, rice, and soybeans account for about 68 per cent of extratropical dry biomass production, so it is likely that the total impact of increased agricultural production exceeds the amount quantified here.

Changes in the seasonality of Northern Hemisphere atmospheric CO_2 concentrations were first noted three decades ago using data from atmospheric monitoring sites at Mauna Loa, Hawaii and Barrow, Alaska[1,7,8]. Parallel evidence from remote sensing, ecosystem models, and eddy covariance measurements have established that Northern Hemisphere extratropical growing seasons have become longer, with concomitant changes in species composition, photosynthetic activity, and ecosystem respiration in boreal and arctic terrestrial ecosystems[4,5,9]. Hence, to explain observed increases in CO_2 seasonality, most studies have focused on the role of climate-induced changes to the terrestrial biosphere in Northern Hemisphere mid- to high latitudes[2,5,6].

Graven *et al.*[3] recently compared Northern Hemisphere atmospheric CO_2 concentrations collected from aircraft around 1960 with similar measurements collected around 2010. Their results not only confirm patterns observed from ground stations, but also reveal a strong latitudinal gradient in changes to the amplitude of CO_2 seasonality, with measurements collected over boreal and arctic regions showing larger increases than measurements collected at lower latitudes. On the basis of the shape of the seasonal CO_2 cycle at higher latitudes, Graven *et al.*[3] suggested that longer growing seasons are insufficient to explain the observed changes in atmospheric CO_2 seasonality, and that enhanced uptake of CO_2 during the middle of the growing season must also be occurring. Consistent with these results, our analyses show that changes in mid-latitude cropland production, with shorter and more intense carbon uptake periods than natural ecosystems[10], and where crop-specific yields have increased by as much as 300% over the past 50 years[11] (Fig. 1), explain a large and previously unrecognized proportion of increases in the seasonality of Northern Hemisphere atmospheric CO_2.

Maize, wheat, rice, and soybeans (MWRS) account for about 64% of global caloric consumption[12] and 58% of global dry biomass production. The bulk of this production occurs in extratropical regions where MWRS represents an even larger share of dry biomass production (68%; Extended Data Tables 1 and 2), and where production has increased 240% since 1965. Remarkably, the harvested area of extratropical MWRS increased less than 18% over this time period, reflecting the fact that production increases were overwhelmingly associated with more productive agricultural practices rather than expansion of cultivated area[13]. Specifically, higher yields were facilitated by development and adoption of improved cultivars and management practices in combination with technological advances, particularly in irrigation and fertilization[12,14,15].

To quantify the contribution of croplands to changes in atmospheric CO_2 seasonality, we developed a carbon accounting methodology that uses gridded time series of MWRS production statistics[13] to calculate MWRS net ecosystem production (NEP) during annual carbon uptake and carbon release periods (CUP and CRP) for the Northern Hemisphere extratropical zones defined by Graven *et al.*[3] (see Methods). In total, extratropical MWRS net primary production (NPP) increased by 0.88 petagrams of carbon (Pg C) between 1961 and 2008, which corresponds to an additional 648 million tonnes of annually harvested biomass. However, since the growing periods for MWRS are not completely in phase with the primary Northern Hemisphere atmospheric CUP (especially in areas supporting multiple cropping and winter wheat), roughly one-quarter of total MWRS productivity occurs during the CRP, thereby mitigating the net impact of total changes in cropland productivity on the seasonality of atmospheric CO_2.

After accounting for the proportions of uptake and release within the CUP and CRP (see Methods), we estimate that changes in Northern Hemisphere extratropical MWRS production increased NEP during the CUP by 0.33 Pg. Since we assume that this carbon is returned to the atmosphere during the CRP, the net effect is an increase in seasonal biosphere–atmosphere carbon exchange of 0.66 Pg C (95% confidence interval 0.49–0.90), from 0.25 Pg C in 1961 to 0.91 Pg C in 2008, a rate of roughly 14 teragrams per year ($Tg\,yr^{-1}$) (Fig. 2a). Graven *et al.*[3] used inverse modelling to quantify the change in seasonal carbon exchange over the same period. Their estimate of 1.3–2.0 Pg C is the additional "seasonal net carbon transfer" (defined as half the sum of carbon assimilated in the CUP and carbon released in the CRP in a net neutral system) over all extratropical lands that is necessary to replicate the observed seasonality enhancement in the atmospheric CO_2 record, accounting for transport and mixing processes. Thus, our results indicate that changes in extratropical production of MWRS accounts for 17%–25% of the enhanced carbon exchange needed to explain the increasing seasonal amplitude of Northern Hemisphere atmospheric CO_2.

Although increases in extratropical MWRS productivity have occurred throughout the Northern Hemisphere (Fig. 3), 88% of the enhanced

---

[1] Department of Earth and Environment, Boston University, Boston, Massachussetts 02215, USA. [2] Earth Systems Research Center, University of New Hampshire, Durham, New Hampshire 03824, USA. [3] Department of Atmospheric, Oceanic and Space Sciences, University of Michigan, Ann Arbor, Michigan 48109, USA. [4] Institute on the Environment, University of Minnesota, Saint Paul, Minnesota 55108, USA. [5] Department of Agronomy and Nelson Institute Center for Sustainability and the Global Environment, University of Wisconsin-Madison, Madison, Wisconsin 53706, USA. [6] Department of Geography, McGill University, Montreal, Quebec H3A 0B9, Canada. †Present address: Liu Institute for Global Issues and Institute for Resources, Environment, and Sustainability, University of British Columbia, Vancouver, British Columbia V6T 1Z2, Canada.

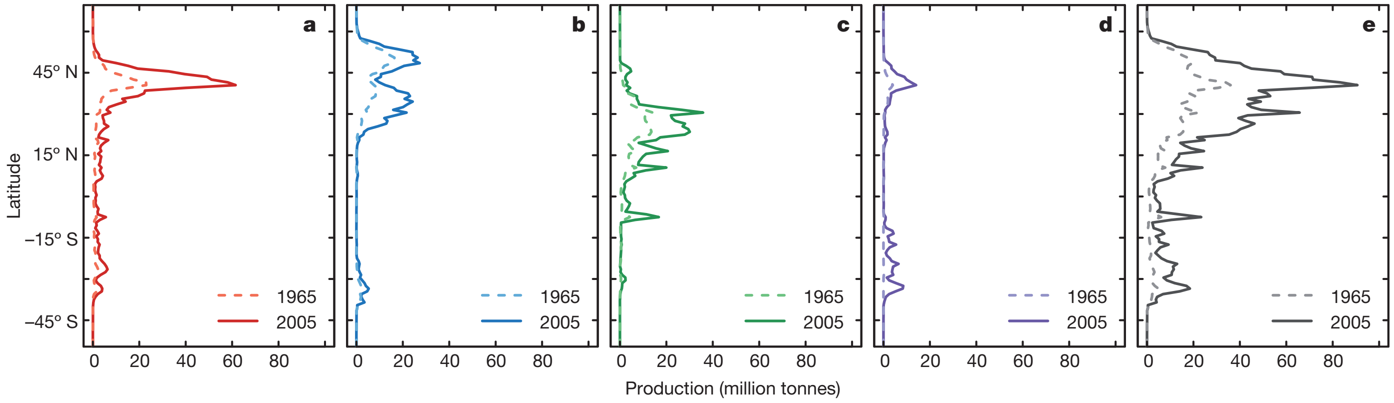

Figure 1 | Latitudinal patterns of increased crop production. Average gridded production values were summed over one-degree latitudinal bands for three-year intervals centred on 1965 and 2005 for maize (**a**), wheat (**b**), rice (**c**), soybeans (**d**) and MWRS (**e**).

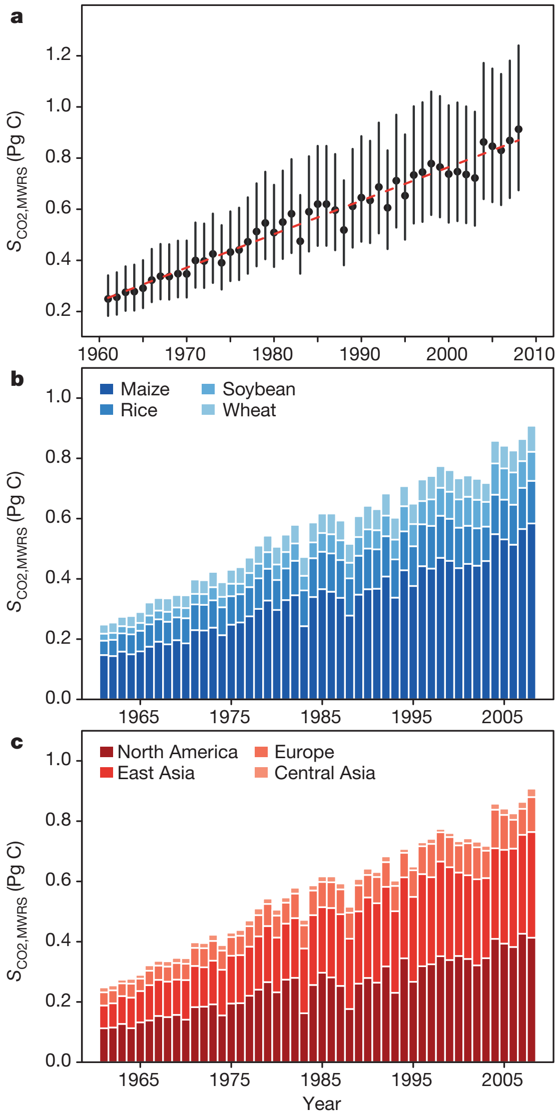

Figure 2 | Attributing the enhanced seasonality. Annual contributions of Northern Hemisphere extratropical MWRS production to atmospheric CO_2 seasonality $S_{CO2,MWRS}$ from 1961 to 2008 with 95% confidence intervals (quantiles from 10^6 iterations) (**a**), contributions to the total increase by crop (**b**), and by region (**c**; see Extended Data Fig. 5). **a** shows a linear fit with a slope of 14 Tg C yr^{-1}.

seasonal carbon exchange due to increased MWRS production is associated with changes in North America (46%, mostly in the United States) and East Asia (42%, mostly in China), where maize is the dominant crop (Figs 2c and 3; Table 1). Further, even though wheat and maize account for similar proportions of total contemporary extratropical MWRS production (34% and 43%, respectively), maize accounts for over 66% of the total change in atmospheric CO_2 seasonality attributable to croplands (Table 1; Fig. 2b). In contrast, wheat explains only 9% of the total change because a substantial proportion of wheat production occurs outside the atmospheric CUP (Extended Data Table 3). Rice accounts for the second largest contribution to increased seasonality (14%; Table 1). However, like wheat, the impact of rice on CO_2 seasonality forcing is relatively minor because a substantial proportion of total rice production occurs outside of the CUP. The role of soybeans is also fairly modest, accounting for 11% of the crop-induced increase in CO_2 seasonality forcing (Fig. 2b).

Crop-specific geographic patterns in MWRS production strongly influence the relative contribution of different regions to total forcing on atmospheric CO_2 seasonality by croplands. Europe, for example, accounts for 38% of contemporary extratropical wheat production and 20% of total extratropical MWRS production, but contributed only 11% to the increase in CO_2 seasonality associated with increased MWRS production (Figs 2c and 3). Total MWRS production is low throughout central Eurasia (Fig. 3), accounting for only 6% of total contemporary extratropical MWRS production. Further, because winter wheat is the dominant crop in this region, central Eurasia accounts for only 2% of the total change in CO_2 seasonality attributable to agriculture (Fig. 2c; Table 1). These results highlight the profound impact that increases in North American and Chinese maize production have had on seasonal carbon budgets of the extratropical Northern Hemisphere.

One of the most remarkable aspects of the changes in cropland productivity we report here is that land used for MWRS production currently occupies less than 6% of vegetated land areas in the extratropical Northern Hemisphere[13]. Thus, increases in CO_2 seasonality associated with MWRS production are being driven almost exclusively by crop management practices and improved genetics that have profoundly transformed the seasonal carbon budgets of intensively managed agroecosystems. Increases in extratropical MWRS production over the past 50 years exceed 240%, whereas model inversions and atmospheric CO_2 records imply that total uptake by terrestrial ecosystems during the extratropical Northern Hemisphere growing season increased only 40%–60% during the same period[3]. Hence, our results indicate that management of agricultural ecosystems occupying a relatively small proportion of land area has had an outsized impact on the seasonality of Northern Hemisphere atmospheric CO_2. Further, most of this contribution occurred in two key regions (northern China and the midwestern USA) via enormous increases in production of a single crop: maize.

Many of the technologies enabling production increases are energy intensive, and are therefore sources of greenhouse gases (for example,

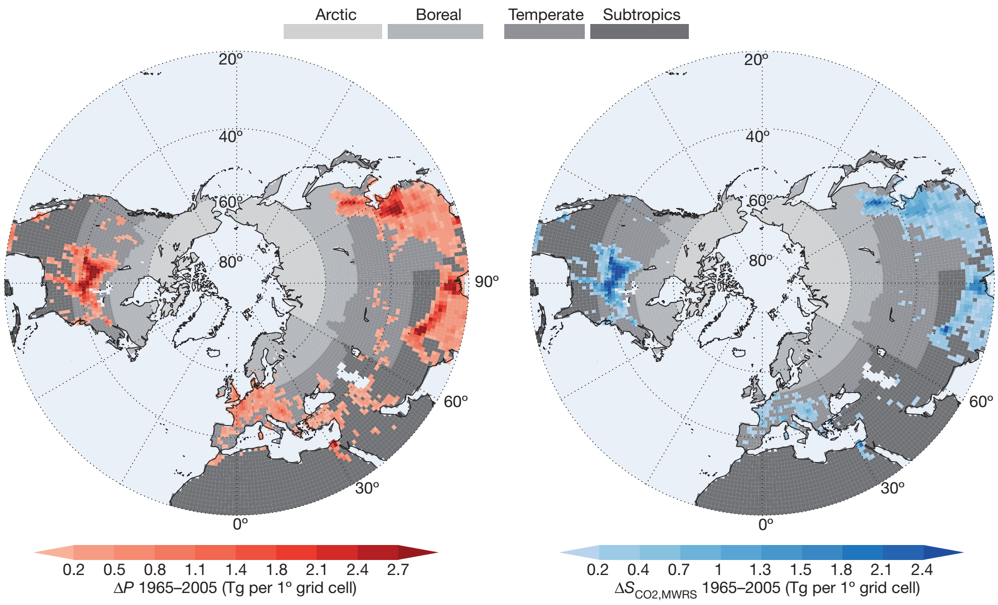

Figure 3 | Increased production and seasonality. Geographic patterns of increases in Northern Hemisphere extratropical MWRS production (P) from 1961–2008 (left), and the resulting increase in forcing to atmospheric CO_2 seasonality (right). Values are shown as sums within 1° × 1° grid cells for illustration, but analyses were conducted at 0.05° × 0.05° grid resolution. Cells with values <0.1 Tg C are not shown (see Extended Data Fig. 6).

fertilizer production, transportation, farm mechanization, and irrigation)[16]. However, CO_2 emissions associated with these technologies are relatively aseasonal, and increases in these emissions over the last 50 years are much smaller than changes in seasonal assimilation of CO_2 arising from increased crop productivity[17]. Similarly, alternative crop residue management practices (for example, no-till) can alter long-term cropland soil carbon source–sink dynamics[18], but have relatively little impact on the seasonality of carbon budgets. Hence, seasonal changes in CO_2 emissions arising from changes in farming technology and practices are small compared to those associated with changes in crop productivity.

Our analysis focused on MWRS because these four crops are the most important and geographically extensive food crops on the planet, and because there are high-quality, global, gridded time series available that allowed us to calculate crop-specific and spatially explicit MWRS NEP[13]. In doing so, however, our analysis excluded roughly 32% of Northern Hemisphere extratropical crop dry-biomass production. Since a large proportion of this unaccounted production occurs in crops with seasonal assimilation patterns that are largely in phase with the Northern Hemisphere CUP, it is likely that the total forcing on atmospheric CO_2 seasonality due to cropland intensification exceeds the contribution from MWRS alone, perhaps substantially so.

Current Earth system models do not replicate observed changes in atmospheric CO_2 seasonality[3,19]. The results presented here suggest that poor representation of agroecosystems within these models explains a substantial proportion of this problem. Indeed, recent results from satellite-borne Sun-induced fluorescence measurements show that both process-based and data-driven models significantly underestimate GPP in croplands, with errors as large as −75% in intensively cultivated areas such as the midwestern USA and the North China plain[20]. Improved representations of contemporary farming practices (fertilization, irrigation, herbicide/pesticide application), multiple cropping, the impact of weeds, pests and diseases on crop physiology and yields, and the higher tolerance of newer cultivars and hybrids to stresses (for example, drought tolerance, flooding) are therefore required for Earth system models to capture geographically and seasonally dependent variations in cropland carbon budgets. In addition to improved process representations, improved data sets that provide spatially and temporally resolved information regarding cropland management practices are also needed.

Table 1 | Percentage of increased extratropical MWRS seasonal carbon exchange by crop and region

Crop	East Asia	North America	Europe	Central Asia	Total
Maize	24	35	7	<1	66
Wheat	3	1	3	1	9
Rice	14	<1	<1	<1	14
Soybeans	2	9	<1	<1	11
Total	42	46	11	2	100

Numerous studies have documented changes in the Northern Hemisphere biosphere over the past several decades[4,9,21–23], but few have explicitly considered the linkage between these changes and increased atmospheric CO_2 seasonality. Changing terrestrial source–sink dynamics related to CO_2 fertilization, growing season length extension, enhanced assimilation/respiration, and biome expansion has been invoked as a primary mechanism leading to the increased atmospheric CO_2 seasonality[1,2,24,25]. Analysis of global carbon budgets point to an increased land sink over the past half-century, although the location of this sink, and the causal mechanisms behind it remain unclear[26–29]. Although it is not inconsistent with these studies, our analysis demonstrates that a substantial portion of increased CO_2 seasonality results from a process that is roughly neutral in terms of its impact on the terrestrial carbon sink. Thus, care must be taken when making inferences regarding the causal linkages between CO_2 seasonality and terrestrial carbon sink dynamics.

By identifying a large and previously unrecognized mechanism that affects atmospheric CO_2 concentrations, the results reported here illuminate an important anthropogenic impact on global carbon budgets, and reveal another pathway through which humans are fundamentally altering the Earth system. In the coming decades, climate change impacts on natural ecosystems are likely to continue, leading to ongoing (and possibly accelerating) intensification of the seasonal cycle of atmospheric CO_2. In parallel, current projections suggest that global food production will need to nearly double over the next 50 years[12,30], requiring concomitant increases in cropland productivity, and by extension, imposing an even stronger signature of human activities in atmospheric CO_2.

Online Content Methods, along with any additional Extended Data display items and Source Data, are available in the online version of the paper; references unique to these sections appear only in the online paper.

Received 6 June; accepted 7 October 2014.

1. Keeling, C., Chin, J. & Whorf, T. Increased activity of northern vegetation inferred from atmospheric CO_2 measurements. *Nature* **382,** 146–149 (1996).

2. Randerson, J., Thompson, M., Conway, T., Fung, I. & Field, C. The contribution of terrestrial sources and sinks to trends in the seasonal cycle of atmospheric carbon dioxide. *Glob. Biogeochem. Cycles* **11,** 535–560 (1997).
3. Graven, H. D. *et al.* Enhanced seasonal exchange of CO_2 by northern ecosystems since 1960. *Science* **341,** 1085–1089 (2013).
4. Piao, S. *et al.* Net carbon dioxide losses of northern ecosystems in response to autumn warming. *Nature* **451,** 49–52 (2008).
5. Elmendorf, S. C. *et al.* Plot-scale evidence of tundra vegetation change and links to recent summer warming. *Nature Clim. Change* **2,** 453–457 (2012).
6. Barichivich, J. *et al.* Large-scale variations in the vegetation growing season and annual cycle of atmospheric CO_2 at high northern latitudes from 1950 to 2011. *Glob. Change Biol.* **19,** 3167–3183 (2013).
7. Bacastow, R., Keeling, C. & Whorf, T. Seasonal amplitude increase in atmospheric CO_2 concentration at Mauna Loa, Hawaii, 1959–1982. *J. Geophys. Res. D* **90,** 10529–10540 (1985).
8. Pearman, G. & Hyson, P. The annual variation of atmospheric CO_2 concentration observed in the Northern Hemisphere. *J. Geophys. Res. Oceans* **86,** 9839–9843 (1981).
9. Xu, L. *et al.* Temperature and vegetation seasonality diminishment over northern lands. *Nature Clim. Change* **3,** 581–586 (2013).
10. Falge, E. *et al.* Seasonality of ecosystem respiration and gross primary production as derived from FluxNET measurements. *Agric. For. Meteorol.* **113,** 53–74 (2002).
11. FAO *FAOSTAT Database* http://faostat.fao.org/ (Food and Agriculture Organization of the United Nations, 2013).
12. Tilman, D., Balzer, C., Hill, J. & Befort, B. L. Global food demand and the sustainable intensification of agriculture. *Proc. Natl Acad. Sci. USA* **108,** 20260–20264 (2011).
13. Ray, D. K., Ramankutty, N., Mueller, N. D., West, P. C. & Foley, J. A. Recent patterns of crop yield growth and stagnation. *Nature Commun.* **3,** 1293 (2012).
14. Kucharik, C. J. Contribution of planting date trends to increased maize yields in the central United States. *Agron. J.* **100,** 328–336 (2008).
15. Mueller, N. D. *et al.* Closing yield gaps through nutrient and water management. *Nature* **490,** 254–257 (2012).
16. Vermeulen, S. J., Campbell, B. M. & Ingram, J. S. I. Climate change and food systems. *Annu. Rev. Environ. Resour.* **37,** 195–222 (2012).
17. West, T. & Marland, G. Net carbon flux from agriculture: carbon emissions, carbon sequestration, crop yield, and land-use change. *Biogeochemistry* **63,** 73–83 (2003).
18. West, T. & Marland, G. A synthesis of carbon sequestration, carbon emissions, and net carbon flux in agriculture: comparing tillage practices in the United States. *Agric. Ecosyst. Environ.* **91,** 217–232 (2002).
19. Keppel-Aleks, G. *et al.* Atmospheric carbon dioxide variability in the community earth system model: evaluation and transient dynamics during the twentieth and twenty-first centuries. *J. Clim.* **26,** 4447–4475 (2013).
20. Guanter, L. *et al.* Global and time-resolved monitoring of crop photosynthesis with chlorophyll fluorescence. *Proc. Natl Acad. Sci.* **111,** E1327–E1333 (2014).
21. Nemani, R. R. *et al.* Climate-driven increases in global terrestrial net primary production from 1982 to 1999. *Science* **300,** 1560–1563 (2003).
22. Chapin, F. *et al.* Role of land-surface changes in Arctic summer warming. *Science* **310,** 657–660 (2005).
23. Goetz, S., Bunn, A., Fiske, G. & Houghton, R. Satellite-observed photosynthetic trends across boreal North America associated with climate and fire disturbance. *Proc. Natl Acad. Sci. USA* **102,** 13521–13525 (2005).
24. McGuire, A. D. *et al.* Carbon balance of the terrestrial biosphere in the twentieth century: analyses of CO_2, climate and land use effects with four process-based ecosystem models. *Glob. Biogeochem. Cycles* **15,** 183–206 (2001).
25. Buermann, W. *et al.* The changing carbon cycle at Mauna Loa observatory. *Proc. Natl Acad. Sci. USA* **104,** 4249–4254 (2007).
26. Angert, A. *et al.* Drier summers cancel out the CO_2 uptake enhancement induced by warmer springs. *Proc. Natl Acad. Sci. USA* **102,** 10823–10827 (2005).
27. Stephens, B. B. *et al.* Weak northern and strong tropical land carbon uptake from vertical profiles of atmospheric CO_2. *Science* **316,** 1732–1735 (2007).
28. Pan, Y. *et al.* A large and persistent carbon sink in the world's forests. *Science* **333,** 988–993 (2011).
29. Le Quéré, C. *et al.* The global carbon budget 1959–2011. *Earth Syst. Sci. Data Discuss.* **5,** 1107–1157 (2012).
30. Foley, J. A. *et al.* Solutions for a cultivated planet. *Nature* **478,** 337–342 (2011).

Acknowledgements This work used eddy covariance data acquired by the FLUXNET community and in particular by the following networks: AmeriFlux (US Department of Energy, Biological and Environmental Research, Terrestrial Carbon Program (DE-FG02-04ER63917 and DE-FG02-04ER63911)), AfriFlux, AsiaFlux, CarboAfrica, CarboEuropeIP, CarboItaly, CarboMont, ChinaFlux, Fluxnet-Canada (supported by CFCAS, NSERC, BIOCAP, Environment Canada, and NRCan), GreenGrass, KoFlux, LBA, NECC, OzFlux, TCOS-Siberia, USCCC. We acknowledge the financial support to the eddy covariance data harmonization provided by CarboEuropeIP, FAO-GTOS-TCO, iLEAPS, Max Planck Institute for Biogeochemistry, National Science Foundation, University of Tuscia, Université Laval and Environment Canada and US Department of Energy and the database development and technical support from Berkeley Water Center, Lawrence Berkeley National Laboratory, Microsoft Research eScience, Oak Ridge National Laboratory, University of California - Berkeley, University of Virginia. This work was supported by NASA grant number NNX11AE75G and NSF grant numbers EF-1064614 and NSF EAR-1038818. Research support to D.K.R. was primarily provided by the Gordon and Betty Moore Foundation and the Institute on Environment at the University of Minnesota. We also acknowledge input and data provided by H. Graven and P. Patra.

Author Contributions J.M.G. led the design, analysis, and writing of the paper. J.M.G., S.F., N.R. and M.A.F. designed the analysis. E.A.K. provided the initial inspiration for the paper and guidance on interpreting atmospheric CO_2 dynamics. C.J.K. contributed guidance on agronomic elements of the paper. D.K.R. provided the gridded MWRS data set. All authors edited and contributed to writing the paper.

Author Information MWRS yield and harvested area data will be archived at http://www.earthstat.org and are available on request. Reprints and permissions information is available at www.nature.com/reprints. The authors declare no competing financial interests. Readers are welcome to comment on the online version of the paper. Correspondence and requests for materials should be addressed to J.M.G. (joshgray@bu.edu).

METHODS

Quantifying cropland S_{CO2}. Seasonality in annual atmospheric CO_2 concentrations arise from the non-uniform temporal distribution of carbon uptake and release by Earth's biotic and abiotic processes. Here we quantify the forcing on Northern Hemisphere (NH) atmospheric CO_2 seasonality due to atmosphere–biosphere carbon exchange (S_{CO2}) as the difference in NEP ($\mathrm{NEP} = -\int \mathrm{NEE}\,dt$) when the net Northern Hemisphere biosphere is a source of carbon to the atmosphere (CRP; $\mathrm{NEE} > 0$) and NEP when the net Northern Hemisphere biosphere is a sink of carbon from the atmosphere (CUP; $\mathrm{NEE} < 0$). Thus $S_{\mathrm{CO2}} = \mathrm{NEP}_{\mathrm{CRP}} - \mathrm{NEP}_{\mathrm{CUP}}$ (Extended Data Fig. 1). Expressing the proportions of annual NPP and R_h that occur during the CUP as θ and φ (that is, $\mathrm{NPP}_{\mathrm{CUP}} = \theta\mathrm{NPP}$ and $R_{\mathrm{h,CUP}} = \varphi\mathrm{NPP}_{\mathrm{CRP}}$), and given that $\mathrm{NEP} = \mathrm{NPP} + R_\mathrm{h}$, after substitution we obtain:

$$S_{\mathrm{CO2}} = [(1-\theta)\mathrm{NPP}(1-\varphi)R_\mathrm{h}] - (\theta\mathrm{NPP} - \varphi R_\mathrm{h}) \qquad (1)$$

Equation (1) may be used to calculate the contribution to S_{CO2} from one component (for example, a single ecosystem) of the carbon cycle, $S_{\mathrm{CO2},i}$, where $S_{\mathrm{CO2}} = \sum_{1}^{n} S_{\mathrm{CO2},i}$ for n components. In this analysis, when calculating S_{CO2}, the CUP is constant across all components (May–August) rather than from the individual component's distinct carbon uptake period. This is because we wish to determine a particular component's forcing on Northern Hemisphere atmospheric CO_2 concentrations, rather than the maximum component-scale difference in NEP. An ecosystem that is assimilating carbon when the net biosphere is releasing carbon would act to weaken (not magnify) the seasonal forcing. Thus, S_{CO2} depends not only on the magnitude of seasonal NEP, but also the degree to which the overall Northern Hemisphere biosphere and individual ecosystem component CUP are in phase. In this analysis, the CUP and CRP were defined as static periods (May–August and September–April, respectively) under the assumption that interannual variations and long-term trends in the timing of atmospheric CO_2 uptake/release were small. This assumption also facilitates comparison with the results of ref. 3 that also assumed a static CUP from 1960 to the present.

Here we calculated the contributions to S_{CO2} from extratropical (see Extended Data Fig. 5) production of maize, wheat, rice, and soybeans ($S_{\mathrm{CO2,MWRS}}$) and considered its change over time: $\Delta S_{\mathrm{CO2,MWRS}} = S_{\mathrm{CO2,MWRS},t2} - S_{\mathrm{CO2,MWRS},t2}$. Assuming that soil carbon changes due to agricultural management, changes in long-term food storage, and the proportion of yield heterotrophically respired out of extratropical regions due to exports are negligible, annual extratropical MWRS NPP ($\mathrm{NPP}_{\mathrm{MWRS}}$) may be assumed to be balanced by annual $R_{\mathrm{h,MWRS}}$ (ref. 31), and $S_{\mathrm{CO2,MWRS}} = 2(\theta - \varphi)\mathrm{NPP}_{\mathrm{MWRS}}$. Further, if θ and φ are constant through time, then $\Delta S_{\mathrm{CO2,MWRS}} = 2(\theta - \varphi)\,\Delta\mathrm{NPP}_{\mathrm{MWRS}}$. We calculate $\mathrm{NPP}_{\mathrm{MWRS},t}$ for a particular time t as the sum of NPP across all crops: $\mathrm{NPP}_{\mathrm{MWRS},t} = \sum_{1}^{k} \mathrm{NPP}_{i,t}$ for k crops.

Converting crop production to total crop NPP. We modified an established approach[32,33] to convert crop production P to total crop carbon (NPP) by way of biophysical parameters describing the biomass carbon fraction (CF, the proportion of dry biomass that is carbon), the harvested biomass moisture fraction (MF, the proportion of harvested biomass that is water), the fraction of grain produced that is harvested (harvest efficiency HE), and biomass partitioning parameters that account for the total root, stem, and leaf biomass production associated with the harvested biomass. The latter may be expressed in terms of the ratio of grain to total above-ground biomass (harvest index, HI), and R:S

$$\mathrm{NPP} = P\left[\frac{\mathrm{CF}(1-\mathrm{MF})}{\mathrm{HE}}\right]\left[\frac{1+R{:}S}{\mathrm{HI}}\right] \qquad (2)$$

Global crop yields and cultivated areas from spatialized national inventory data[14] were used to calculate P for MWRS for the period 1961–2008. We assumed a constant carbon fraction of dry biomass of carbon fraction = 0.45 (ref. 33), and an average MWRS moisture content of $\overline{\mathrm{MF}} = 0.105$ with a range of 0.09–0.11 from the literature[33]. Harvest efficiency accounts for a variety of factors that reduce actual yields from their potential, including combine efficiency, herbivory, and crop failures. Lacking detailed data on these processes, we assumed a very conservative value for harvest efficiency (0.97), representing the maximum value for industrialized crop production, and adopted a range for harvest efficiency of 0.9–0.97 with a most likely value of 0.95. Since harvest efficiency in less industrialized and technologically advanced production regimes is probably lower, and there is some non-negligible amount of non-harvested or failed crops, we stress that this is a conservative estimate (favouring lower amounts of total production) for harvest efficiency.

We compiled 86 values of harvest index for MWRS[34–43], and 24 values of R:S reported in the literature[34,39,44–50], and analysed their distributions. The average reported harvest index across all crops was 0.42 and ranged from 0.17 to 0.62 (Extended Data Fig. 2a). An F-test did not support there being a significant difference between crop-specific values of harvest index ($P = 0.57$). Therefore, we used a single harvest index distribution for all crops, and defined it by the most-likely value (the harvest index mean is 0.42), and the range containing 95% of the data (0.2–0.6). Owing mostly to challenges in accurately measuring total root biomass[39], there is high variability in the literature values of R:S. As with harvest index, our data showed no significant difference between R:S among MWRS ($P = 0.62$), so we adopted a common distribution defined by the mean value 0.35, and a broad range of variability: 0.1–0.7 (Extended Data Fig. 2b). The goal of this exercise was not to provide a rigorous metanalysis of harvest index and R:S values reported in the literature, but rather to characterize a realistic and defensible distribution of these parameters for the crops of interest.

There is modest literature and theoretical support for harvest index increasing for certain crops over time, owing mostly to dwarfing varieties of wheat and rice[34]. For example, Hay *et al.*[34] reported increases in wheat and rice harvest index of 0.05–0.1 over the period 1960–1990, but stable harvest index for maize. Johnson *et al.*[39] assumed an increase from 0.35 to 0.53 for maize, and from 0.28 to 0.45 for wheat over the period 1940–2000. In contrast, Lorenz *et al.*[41] analysed five studies growing maize varieties from different eras and found that four out of the five did not have a significant change in harvest index over time. We found no support for increasing harvest index across all crops in our data set, although the relative paucity of data before 1980 prohibited a definitive analysis. However, given the disagreement between existing studies, the difficulties in drawing conclusions about changes in harvest index from historical crop varieties grown in modern conditions, and the relatively modest reported increases, we used temporally static distributions for harvest index in this study.

Our analysis assumes that parameters controlling biomass partitioning in crops (that is, harvest index and R:S) were constant. Cultivars that preferentially partition assimilated carbon to grain (for example, dwarfed varieties of wheat and rice) violate this assumption, and widespread adoption of these crops would introduce bias to our results. However, analysis of available crop data suggest that changes in harvest index and R:S for wheat and rice between 1960–2010 were insignificant. Further, changes in productivity for maize and soybean, which have no dwarfed equivalents, account for 77% of the total MWRS contribution to increased atmospheric CO_2 seasonality, such that allowing the harvest index for wheat and rice to increase by 30% reduces our estimate of the MWRS forcing on atmospheric CO_2 by only 2%. Hence, our assumption of invariance in harvest index and R:S appears to be robust.

An assessment of the uncertainty in the gridded production data of ref. 15, or of the FAO data from which these data are derived, has not been undertaken. How well production statistics reflect actual production amounts probably varies across reporting units and depends on the technological and logistical capacity to undertake the large-scale data collection and processing efforts necessary to produce high-quality estimates. Although a detailed assessment of this uncertainty would theoretically be possible for small areas, we are not aware of any efforts to do so. Nevertheless, we assessed the effect of variable levels of uncertainty on the 95% confidence intervals of our change in seasonality estimate. To do so, we assumed that the annual production totals may be subject to $\pm N$% errors drawn from a uniform distribution. Since the change in seasonality is approximately linear with changes in NPP (see equation (1)), the confidence intervals broaden with increasing uncertainty N at a rate of 0.006 Pg C per 1% increase in uncertainty. Thus, if the total production values were within 10% of the true value, the 95% confidence interval of our estimate increases from 0.50–0.90 to 0.47–0.92, and to 0.41–1.00, assuming ±30% errors. We note that the majority of the MWRS production considered in this study occurred in developed countries with ample capacity to provide accurate estimates. Coupled with the economic value in obtaining and reporting accurate statistics, this fact suggests that production uncertainties are probably low.

Assimilation proportion in CUP, θ. The temporal partitioning of crop NPP into proportions occurring when net Northern Hemisphere ecosystems are assimilating carbon (CUP) and releasing carbon (CRP) is dependent on crop-specific sowing and harvest dates and developmental phenology. We employed two different approaches to determining θ for the crops in this study: analysis of eddy-covariance flux data, and the use of global crop calendars with assumptions about the distribution of NPP between sowing and harvest dates. In applying our model of the change in seasonality, crop-specific values of θ are assumed to be constant through time. Note, however, that specifying θ on a crop-specific basis means that the composite MWRS value of θ will be responsive to changes in the relative production of crops through time.

The FluxNET "free and fair use dataset"[51] contains eddy-covariance flux data for several agricultural sites throughout the world. Subsets of these data include only complete years for four sites in the USA: US-Bo1, US-Ne1, US-Ne2, and US-Ne3, comprising 22 full years of measurements over maize and soybean crops under various irrigation and tillage management protocols (Extended Data Fig. 3). We assumed that GPP and NPP were proportional throughout the growing period (that is, autotrophic respiration was a static proportion of GPP)[52], and estimated θ by calculating the proportion of FluxNET-modelled GPP falling within the atmospheric CUP for each year across sites. The median value of θ across all site years was 0.85, and all values were in the range 0.72–0.93. We found no statistically significant difference between θ values for maize and soybean rotations (Student's *t*-test $P = 0.39$). Therefore, we adopted the range 0.72–0.93 and a most likely value of 0.85 for the distributions of both θ_{maize} and $\theta_{\mathrm{soybean}}$. We assumed that these USA-based values are representative of maize and soybean production throughout the Northern Hemisphere on the basis of the congruence of crop calendars in China/East Asia and North America (Extended Data Table 3), and the similarity of climatic forcing throughout these regions.

We adopted a different approach to determining θ_{rice} and θ_{wheat}, owing to the lack of available full-year eddy-covariance flux data for these crops. Additionally, these crops have unique challenges in defining θ due to winter versus spring wheat, and their prevalence in multicropping rotations[53]. For these reasons, we relied on global crop calendars[54] (Extended Data Table 3) providing typical sowing and harvest dates, and assumptions about the temporal distribution of NPP within the crop growing seasons. We assumed that root and non-harvested aboveground biomass is created entirely during the crop's vegetative growth phase, that the grain portion of NPP is created entirely during the following reproductive growth phase[55], and that NPP is accumulated at a constant rate within each of these periods. We defined the reproductive growth phase of wheat and rice as the final 40 days before harvest and calculated the proportion of crop biomass that was created during the atmospheric CUP.

Nearly 97% of all the rice produced in the temperate zone is produced in China and East Asia[12]. Modes of Chinese rice production vary with geography. In the north, where temperature is a limiting factor, production typically occurs in single-crop rotations or in double rotations of winter wheat and summer rice. In the south, where multicropping rotations dominate, rice is typically one or two of the two or three crops grown in various rotations throughout the region. We used maps of Chinese rice rotations and associated areas[56] to characterize the relative magnitudes of rice produced during various growing seasons. These data indicate that 72% of Chinese rice production occurs during the main growing season. Since triple-cropped rice contributes a small fraction of the overall production, we assumed that the remaining 28% of rice production conforms to the sowing and harvest dates for the second rice crop. Thus, using the sowing and harvest dates for the first and second rice crops, and the abovementioned assumptions about temporal partitioning of biomass between vegetative and reproductive growth phases, we calculated the proportion of rice production occurring in the CUP as the sum of the products of the first or second rice crop production proportion and the corresponding average proportion of production in CUP to be $(0.72 \times 0.90) + (0.28 \times 0.355) = 0.75$. Continuing in this fashion for the minimum and maximum during-CUP production portions, we arrived at a range for during-CUP rice production of 0.65–0.84, and a most likely value of 0.75.

Calculating θ_{wheat} presented similar challenges because of differences in the growing seasons, and relative production magnitudes, of winter and spring wheat varieties. In the USA, winter wheat varieties account for about 70% of production. Using areas of double- and triple-cropping[57], and assuming that all double- and triple-cropped wheat is a winter variety, and that all single-cropped wheat is a spring variety, we conclude that winter varieties account for 64% of Chinese wheat production. The fraction is lower in Canada owing to the harsher winters, and the same or higher throughout Europe. Therefore, we assumed that the global winter/spring wheat proportions followed that of the USA, and calculated the proportion of winter and spring wheat NPP occurring in the CUP as for rice, arriving at a most likely value for θ_{wheat} of 0.52 and a likely range of 0.47–0.57. For comparison, calculating θ_{maize} and $\theta_{\mathrm{soybean}}$ on the basis of crop calendars rather than eddy-covariance data, we arrive at very similar range for θ_{maize} of 0.72–0.88, with a most likely value of 0.80, and for $\theta_{\mathrm{soybean}}$ a range of 0.79–0.86, with a most likely value of 0.83. Thus, the two methods have reasonable agreement, bolstering our confidence in the estimates of θ_{wheat} and θ_{rice}. Future efforts may seek to define these parameters on the basis of satellite observations of growing season timing, which clearly show that agricultural lands have shorter photosynthetically active periods than do natural ecosystems (Extended Data Fig. 7).

Respiration proportion in CUP, φ. As with θ, we relied on analysis of eddy-covariance flux data to determine the proportion of respiration occurring in the CUP, φ. Since our calculation of crop NPP accounts for autotrophic respiration, φ should be the proportion of R_{h} of crop residues occurring in the CUP, rather than the total respiration. We assumed that R_{h} occurs across two pools: grain biomass (φ_{g}), and root/shoot/leaves/and so on (φ_{rs}). The respiration from grain occurs due to human and animal consumption of grain biomass, and was assumed to occur evenly throughout the year. Thus, φ_{g} was assumed to be constant across crops and equivalent to the proportion of the year occupied by the CUP, or one-third. As with θ, all φ parameters were assumed to be constant through time.

Calculating φ_{rs} required partitioning the FluxNET-estimated total ecosystem respiration into heterotrophic and autotrophic proportions. Autotrophic respiration dominates total respiration during crop growth, accounting for 40%–60% of GPP[52]. Aubinet *et al.*[52] analysed eddy-covariance data, soil chambers, and biomass measurements to estimate the autotrophic to total respiration fraction and found that in no case was the fraction lower than 0.65. Here, we assumed that the ratio of autotrophic to total ecosystem respiration during the growing season was in the range 0.65–0.85, and used that information to partition the FluxNET-estimated total ecosystem respiration into autotrophic and heterotrophic components. Then, as with θ, we estimated φ_{rs} as the proportion of total annual R_{h} that occurs during the CUP. In this way we determined that φ_{rs} is probably in the range 0.36–0.68 with a most likely value of 0.5. Since the rate of R_{h} is largely determined by climate, we assume that these values are representative for all crops in this study.

Estimating $S_{\mathrm{CO2,MWRS}}$ and $\Delta S_{\mathrm{CO2,MWRS}}$. We used equations (1) and (2) to calculate annual values of $S_{\mathrm{CO2,MWRS}}$, and accounted for parameter uncertainty by adopting a Monte Carlo approach. Parameter values were specified by PERT distributions (special case of a beta distribution) using the minimum, maximum, and most likely values previously specified (Extended Data Fig. 4). Carbon fraction and φ_{g} were assumed to have constant values for all simulations. $S_{\mathrm{CO2,MWRS}}$ in each year was calculated from 1×10^{6} parameter set realizations. The change in the forcing of MWRS production on atmospheric carbon seasonality $\Delta S_{\mathrm{CO2,MWRS}}$ was calculated as the difference between $S_{\mathrm{CO2,MWRS}}$ in 1961 and in 2008, the endpoints of our global production data.

Soil carbon and production-related emissions. Non-crop CO_2 emissions associated with MWRS production were not explicitly considered in this study. However, extrapolating the average USA values of agriculture-associated carbon emissions to the globe (accounting for the full life-cycle emissions associated with agricultural inputs: production, transport, application, irrigation, farm machinery and so on)[24], we determined that the likely upper limit of carbon emissions associated with the total global production of agricultural crop is about 0.2 Pg C yr^{-1}. However, as with the R_{h} of biomass, the impact of these emissions on atmospheric CO_2 seasonality depends on the temporal partitioning of emissions into CUP and CRP components, with during-CUP emissions offsetting the additional assimilated carbon, and emissions in the CRP enhancing the total flux of carbon to the atmosphere. Considering that many of the dominant components of these emissions are not strongly seasonal (such as the production and transport of agricultural inputs), and that the most emissions-intensive during-CUP process is irrigation, which accounts for a small percentage of total cultivated area (15% in the United States), we can assume that the imbalance between the CUP and CRP proportions of emissions is probably small, but slightly favours during-CUP emissions. Further, actual emissions for temperate production of crops are probably considerably less than the calculated global maximum value of 0.2 Pg C yr^{-1} because these crops represent only a fraction of the global production of all crops. Thus, we conclude that the unaccounted-for carbon emissions associated with agricultural production most probably leads to a modest reduction only in the estimated contribution of increased agricultural production to the seasonality of atmospheric CO_2 concentrations, although this contribution may increase with the expansion of irrigation.

Changes in soil carbon due to agricultural production were also not calculated here, despite the fact that agricultural production has the potential to alter soil carbon source/sink dynamics with a magnitude dependent mostly on the management of crop residues[24,58]. In the context of atmospheric carbon seasonality, increased soil carbon storage would reduce the amount of CUP-assimilated carbon returned to the atmosphere during the CRP, and therefore diminish the impact on atmospheric CO_2 seasonality. However, the amount of carbon sequestered in croplands is generally less than 2% of NPP[31], and therefore soil carbon changes have low potential to affect seasonality on an annual timescale. Additional unaccounted-for emissions of carbon associated with land-use conversion for agriculture may contribute significantly to global carbon source/sink dynamics owing to the release of long-term carbon stores[59], but probably contributes very little to the seasonality of atmospheric CO_2 because of the relatively small magnitude of the extratropical increase in MWRS area (only about 18% expansion in this time frame). Further, total extratropical harvested area actually decreased 2% over this time period[12], meaning that it is likely that MWRS expansion has been on existing croplands.

31. West, T. O., Bandaru, V., Brandt, C. C., Schuh, A. E. & Ogle, S. M. Regional uptake and release of crop carbon in the United States. *Biogeosciences* **8,** 2037–2046 (2011).
32. Prince, S., Haskett, J., Steininger, M., Strand, H. & Wright, R. Net primary production of US midwest croplands from agricultural harvest yield data. *Ecol. Appl.* **11,** 1194–1205 (2001).
33. Lobell, D. *et al.* Satellite estimates of productivity and light use efficiency in united states agriculture, 1982-98. *Glob. Change Biol.* **8,** 722–735 (2002).
34. Hay, R. Harvest index—a review of its use in plant-breeding and crop physiology. *Ann. Appl. Biol.* **126,** 197–216 (1995).
35. Sinclair, T. Historical changes in harvest index and crop nitrogen accumulation. *Crop Sci.* **38,** 638–643 (1998).

36. Kumudini, S., Hume, D. & Chu, G. Genetic improvement in short season soybeans: I. dry matter accumulation, partitioning, and leaf area duration. *Crop Sci.* **41,** 391–398 (2001).
37. Wirsenius, S. Efficiencies and biomass appropriation of food commodities on global and regional levels. *Agric. Syst.* **77,** 219–255 (2003).
38. Shearman, V., Sylvester-Bradley, R., Scott, R. & Foulkes, M. Physiological processes associated with wheat yield progress in the UK. *Crop Sci.* **45,** 175–185 (2005).
39. Johnson, J. M. F., Allmaras, R. R. & Reicosky, D. C. Estimating source carbon from crop residues, roots and rhizodeposits using the national grain-yield database. *Agron. J.* **98,** 622–636 (2006).
40. Haberl, H. *et al.* Quantifying and mapping the human appropriation of net primary production in earth's terrestrial ecosystems. *Proc. Natl Acad. Sci. USA* **104,** 12942–12947 (2007).
41. Lorenz, A. J., Gustafson, T. J., Coors, J. G. & de Leon, N. Breeding maize for a bioeconomy: a literature survey examining harvest index and stover yield and their relationship to grain yield. *Crop Sci.* **50,** 1–12 (2010).
42. Ma, S.-C., Li, F.-M., Xu, B.-C. & Huang, Z.-B. Effect of lowering the root/shoot ratio by pruning roots on water use efficiency and grain yield of winter wheat. *Field Crops Res.* **115,** 158–164 (2010).
43. Yang, J. & Zhang, J. Crop management techniques to enhance harvest index in rice. *J. Exp. Bot.* **61,** 3177–3189 (2010).
44. Gower, S. T., Kucharik, C. J. & Norman, J. M. Direct and indirect estimation of leaf area index, fAPAR, and net primary production of terrestrial ecosystems. *Remote Sens. Environ.* **70,** 29–51 (1999).
45. Bonifas, K., Walters, D., Cassman, K. & Lindquist, J. Nitrogen supply affects root: shoot ratio in corn and velvetleaf (*Abutilon theophrasti*). *Weed Sci.* **53,** 670–675 (2005).
46. Insalud, N., Bell, R. W., Colmer, T. D. & Rerkasem, B. Morphological and physiological responses of rice (*Oryza sativa*) to limited phosphorus supply in aerated and stagnant solution culture. *Ann. Bot.* **98,** 995–1004 (2006).
47. Jing, L., Shi-Qing, L., Yi, L. & Xiao-Li, C. Effects of increased ammonia on root/shoot ratio, grain yield and nitrogen use efficiency of two wheat varieties with various N supply. *Plant Soil Environ.* **55,** 273–280 (2009).
48. Arai-Sanoh, Y., Ishimaru, T., Ohsumi, A. & Kondo, M. Effects of soil temperature on growth and root function in rice. *Plant Prod. Sci.* **13,** 235–242 (2010).
49. Gehring, C. *et al.* Ecological intensification of rice production in the lowlands of Amazonia—options for smallholder rice producers. *Eur. J. Agron.* **46,** 25–33 (2013).
50. Williams, J. D. *et al.* Root:shoot ratios and belowground biomass distribution for pacific northwest dryland crops. *J. Soil Water Conserv.* **68,** 349–360 (2013).
51. FluxNET http://www.fluxdata.org (2014).
52. Aubinet, M. *et al.* Carbon sequestration by a crop over a 4-year sugar beet/winter wheat/seed potato/winter wheat rotation cycle. *Agric. For. Meteorol.* **149,** 407–418 (2009).
53. Dawe, D., Frolking, S. & Li, C. Trends in rice-wheat area in China. *Field Crops Res.* **87,** 89–95 (2004).
54. Sacks, W. J., Deryng, D., Foley, J. A. & Ramankutty, N. Crop planting dates: an analysis of global patterns. *Glob. Ecol. Biogeogr.* **19,** 607–620 (2010).
55. Schnyder, H. The role of carbohydrate storage and redistribution in the source-sink relations of wheat and barley during grain filling—a review. *New Phytol.* **123,** 233–245 (1993).
56. Frolking, S. *et al.* Combining remote sensing and ground census data to develop new maps of the distribution of rice agriculture in China. *Glob. Biogeochem. Cycles* **16,** 1091 (2002).
57. Qiu, J. *et al.* Mapping single-, double-, and triple-crop agriculture in China at 0.5x0.5 by combining county-scale census data with remote sensing-derived land cover map. *Geocarto Int.* **18,** 3–13 (2003).
58. Baker, J. M., Ochsner, T. E., Venterea, R. T. & Griffis, T. J. Tillage and soil carbon sequestration—what do we really know? *Agric. Ecosyst. Environ.* **118,** 1–5 (2007).
59. DeFries, R., Field, C., Fung, I., Collatz, G. & Bounoua, L. Combining satellite data and biogeochemical models to estimate global effects of human-induced land cover change on carbon emissions and primary productivity. *Glob. Biogeochem. Cycles* **13,** 803–815 (1999).

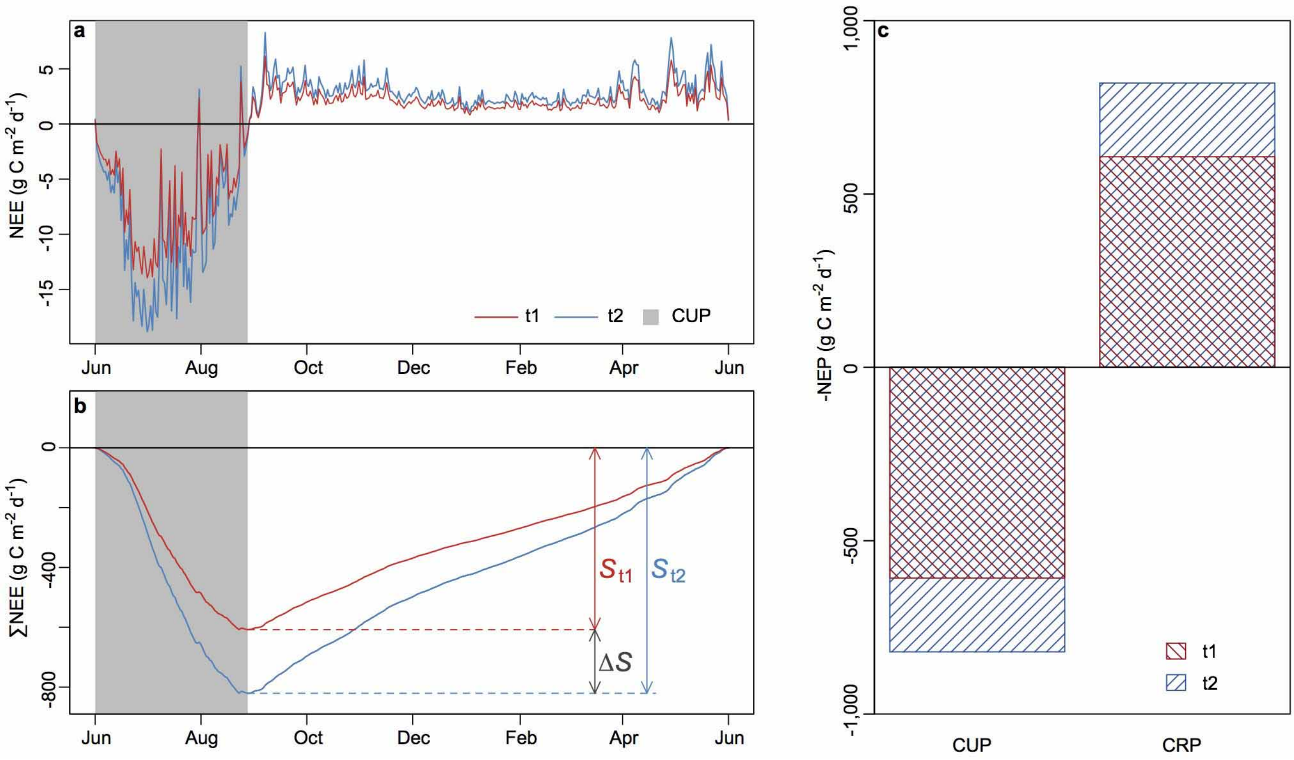

Extended Data Figure 1 | Calculating Δ*S*. Schematic diagram showing the CO_2 seasonality difference (ΔS) for two time periods representing a baseline condition (*t*1) with CO_2 seasonality S_{t1} and a scenario where NEE is enhanced 35% (*t*2) with correspondingly higher seasonality, S_{t2}. Flux-derived daily NEE (**a**), cumulative NEE (**b**), and NEP_{CUP} and NEP_{CRP} (**c**). Note the assumption that annual NEP = 0 (**b**).

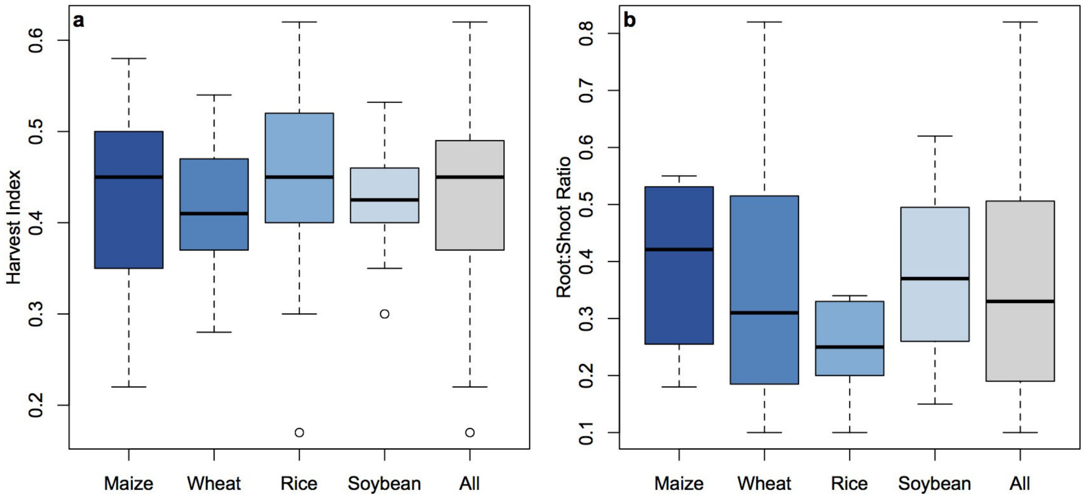

Extended Data Figure 2 | Harvest index and root:shoot ratio. Crop-specific and MWRS aggregate distributions of literature-reported values of harvest index (**a**) and *R*:*S* (**b**).

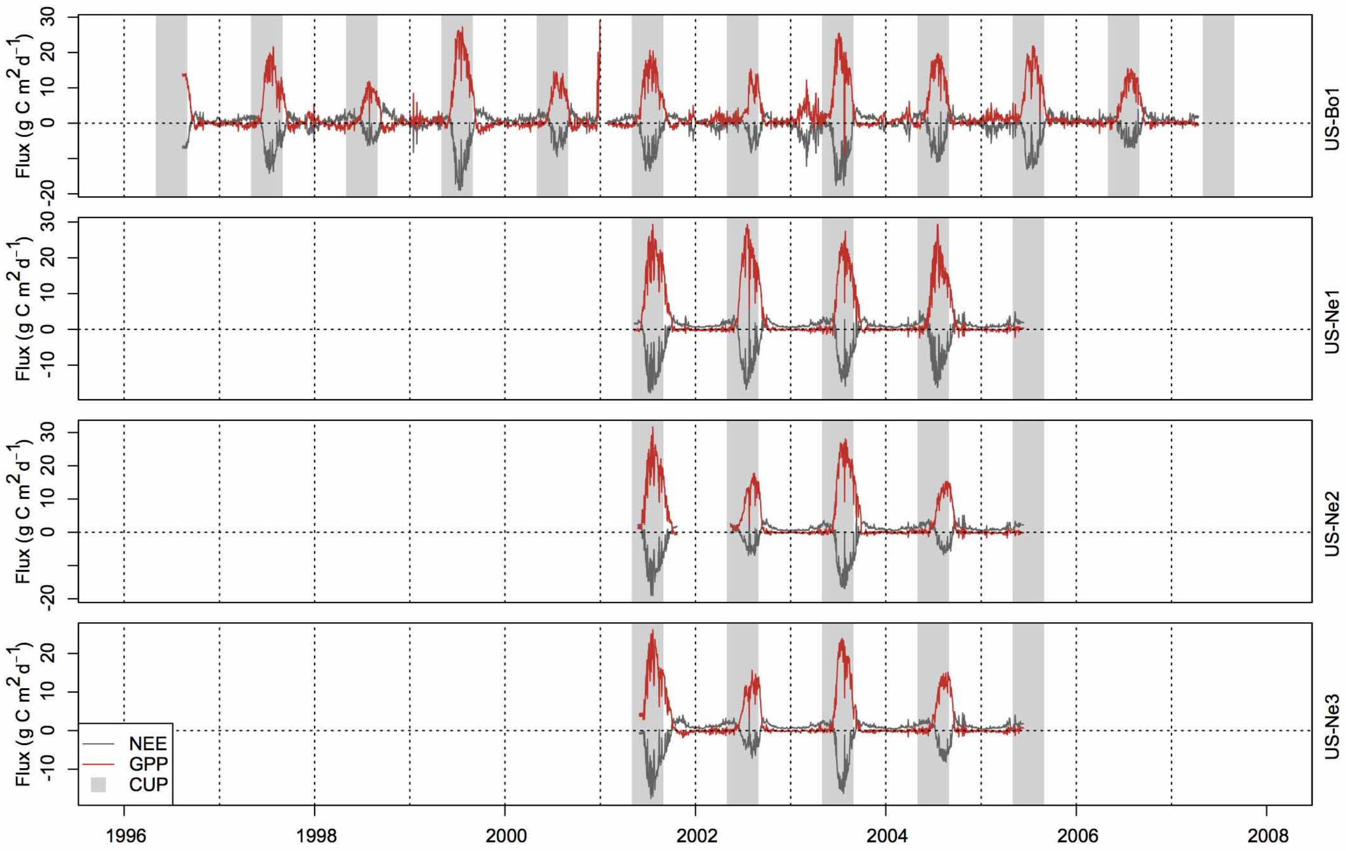

Extended Data Figure 3 | Agricultural fluxes from FluxNET. NEE and GPP for agricultural FluxNET sites used in this study to determine the θ and φ parameters. Shading corresponds to May, June, July, and August, the CUP at the latitudes of most agricultural production, and the CUP definition used throughout this study.

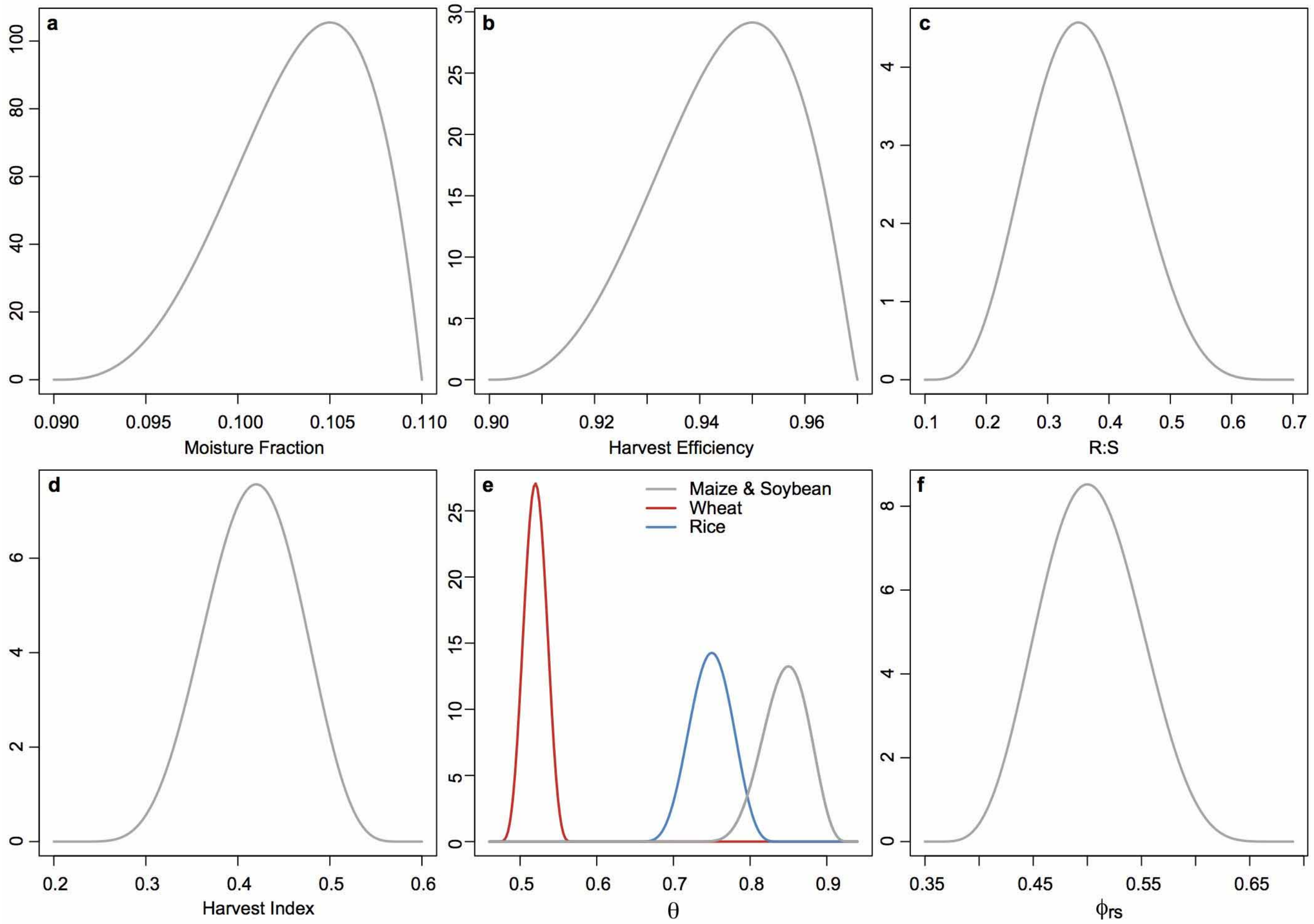

Extended Data Figure 4 | Parameter distributions. PERT distributions for all Monte-Carlo-varied parameters in this study. Shown are moisture fraction (**a**), harvest efficiency (**b**), *R*:*S* ratio (**c**), harvest index (**d**), CUP proportion of NPP (**e**), and CUP proportion of R_h (**f**).

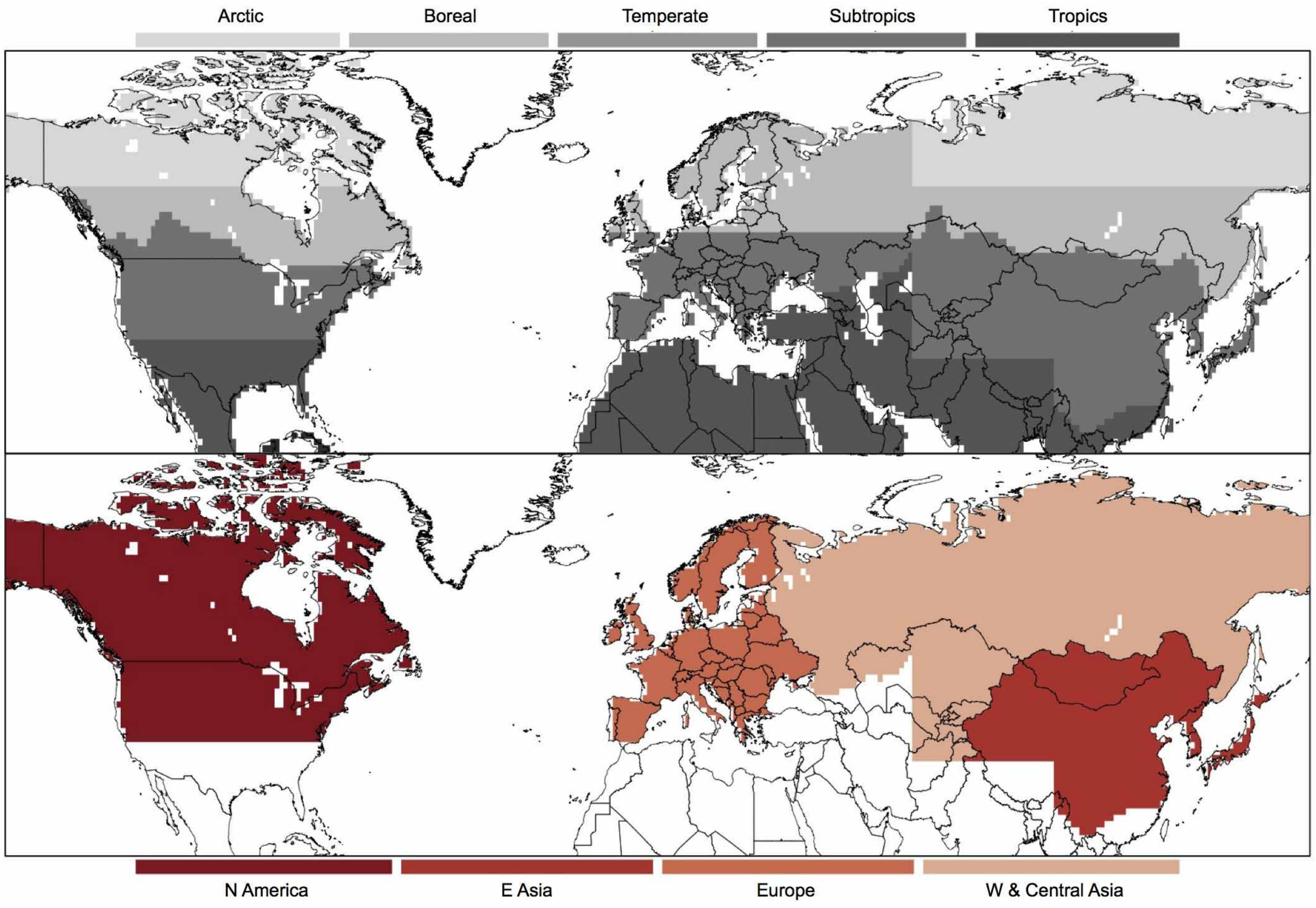

Extended Data Figure 5 | Aggregation zones. Eco-climatic (top; from ref. 3) and aggregated production regions (bottom) used in this study.

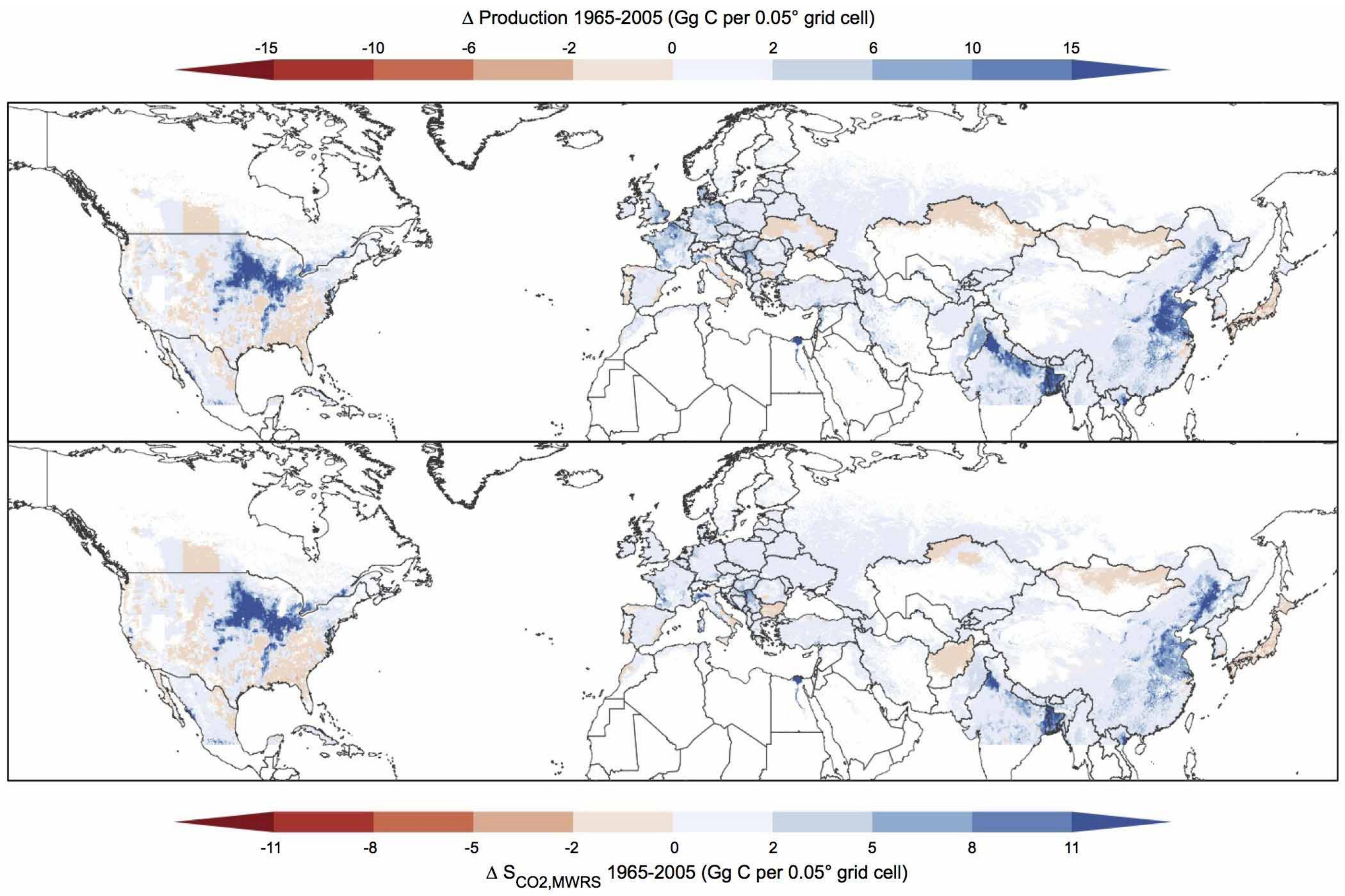

Extended Data Figure 6 | Increased production and seasonality. Change in MWRS production (top) and $S_{\mathrm{CO2,MWRS}}$ (bottom) over the period 1965–2005.

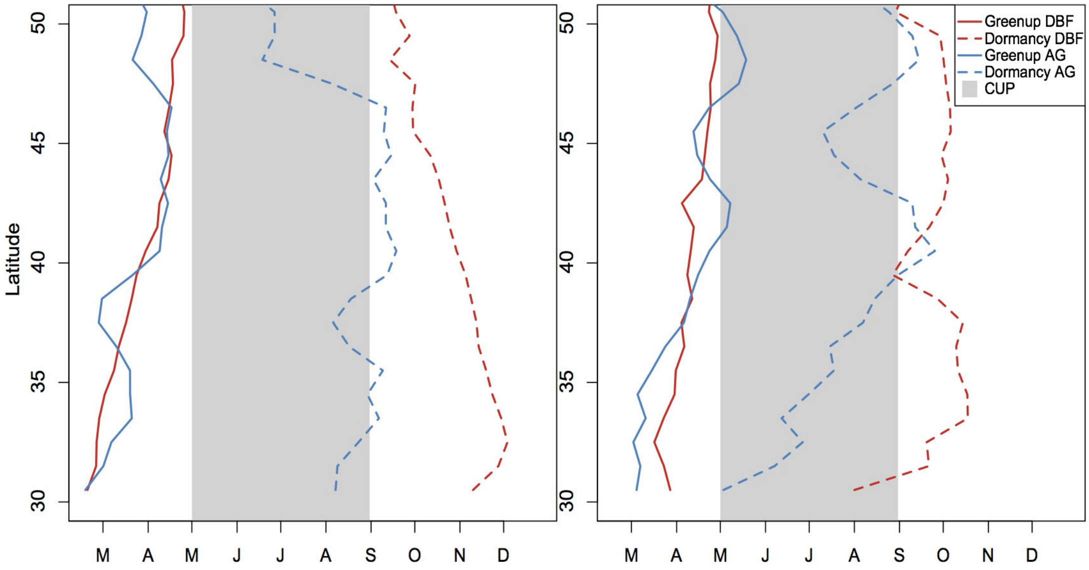

Extended Data Figure 7 | Remotely sensed growing season length. Mean 'greenup' and dormancy values from MODIS Land Cover Dynamics product (MCD12Q2) for pixels identified as agriculture (AG) and deciduous broadleaf forest (DBF) in the MODIS Land Cover product (MCD12Q1; classes 12 and 4, respectively) for 1° latitudinal bands in North America (**a**) (MODIS tiles are h11v03, h12v03, h13v03, h10v04, h11v04, h12v04, h09v05, h10v05, and h11v05), and for China (**b**) (MODIS tiles are h23v03, h24v03, h25v03, h26v04, h27v04, h26v05, and h27v05.)

Extended Data Table 1 | Global dry biomass production

Crop	Production	1 - MF	Dry Biomass	Fraction of Total	Cumulative Fraction
Maize	872	0.895	780	0.199	0.199
Rice, paddy	720	0.895	644	0.165	0.364
Wheat	671	0.895	600	0.153	0.517
Sugar cane	1,833	0.15	275	0.070	0.587
Soybeans	242	0.895	216	0.055	0.643
Palm Oil	250	0.8	200	0.051	0.694
Barley	133	0.895	119	0.030	0.724
Potatoes	365	0.28	102	0.026	0.750
Cassava	263	0.32	84	0.022	0.772
Seed cotton	77	0.92	70	0.018	0.790
Sorghum	57	0.89	51	0.013	0.803
Coconuts	60	0.8	48	0.012	0.815
Rapeseed	65	0.73	47	0.012	0.827
Cottonseed	47	0.92	43	0.011	0.838
Palm Oil (fruit)	50	0.8	40	0.010	0.848
Groundnuts (with shell)	41	0.92	38	0.010	0.858
Sunflower seed	37	0.94	35	0.009	0.867
Fresh Vegetables, various	270	0.13	35	0.009	0.876
Sugar beet	270	0.12	32	0.008	0.884
Millet	30	0.9	27	0.007	0.891
Sweet potatoes	103	0.25	26	0.007	0.898
Cotton lint	26	0.92	24	0.006	0.904
Beans, dry	24	0.9	21	0.005	0.909
Bananas	102	0.2	20	0.005	0.914
Oats	21	0.89	19	0.005	0.919
Yams	59	0.3	18	0.005	0.924
Olives	17	0.8	13	0.003	0.927
Rye	15	0.88	13	0.003	0.930
Grapes	67	0.19	13	0.003	0.934
Triticale	14	0.9	12	0.001	0.937
Apples	76	0.16	12	0.003	0.940
Palm kernels	15	0.8	12	0.003	0.943
Onions, dry	83	0.13	11	0.003	0.946
Chick peas	12	0.9	10	0.003	0.948
Tomatoes	162	0.06	10	0.003	0.951
Watermelons	105	0.09	9	0.002	0.953
Rubber, natural	11	0.8	9	0.002	0.956
Oranges	68	0.13	9	0.002	0.958
Peas, dry	10	0.9	9	0.002	0.960
Mangoes & guavas	42	0.18	8	0.002	0.962
Plantains	37	0.2	7	0.002	0.964
Coffee (green)	9	0.8	7	0.002	0.966
Tobacco, unmanufactured	7	0.8	6	0.002	0.967
Fresh Fruit, various	31	0.19	6	0.002	0.969
Cabbages & similar	70	0.08	6	0.001	0.970
Cow peas (dry)	6	0.9	5	0.001	0.972
Tangerines & similar	27	0.19	5	0.001	0.973
Other Cereals	6	0.88	5	0.001	0.974
Pumpkins, squash & gourds	25	0.2	5	0.001	0.975
Pulses	5	0.9	5	0.001	0.977
Carrots & turnips	37	0.12	4	0.001	0.978
Lentils	5	0.89	4	0.001	0.979
Cocoa (beans)	5	0.8	4	0.001	0.980
Other Grains	5	0.88	4	0.001	0.981
Tropical Fresh Fruit	20	0.19	4	0.001	0.982
Eggplants	48	0.08	4	0.001	0.983
Tea	5	0.8	4	0.001	0.984
Pigeon peas	4	0.9	4	0.001	0.985
Broad & horse beans (dry)	4	0.9	4	0.001	0.986
Pears	24	0.16	4	0.001	0.987

Global production and dry biomass (in megatonnes), dry biomass fraction (1 − moisture fraction), and the crop-specific and cumulative fraction around 2012 for all crops accounting for greater than 0.1% of total harvested dry biomass.

Extended Data Table 2 | 2009–2011 mean MWRS dry biomass production

Region	Maize	Wheat	Rice	Soybeans	MWRS	MWRS fraction
Eastern Asia	161	105	195	13.9	475	0.68
North America	297	75	9	83	463	0.85
Europe	83	195	4	4	287	0.54
Central Asia	1	24	1	0	26	0.62
Western Asia	5	27	1	0	33	0.50
Extratropical total	547	426	210	101	1,280	0.68
Global	763	608	631	224	2,226	0.58

'MWRS fraction' is the MWRS production fraction of total production (in Tg) for all crops for which we have moisture fraction data (see Extended Data Table 1), which is the majority of total crop production in each region (99.2% for Eastern Asia, 99.6% for North America, 99.0% for Europe, 96.9% for Western Asia, and 98.6% for Central Asia.

Extended Data Table 3 | Proportion of NPP in CUP

Crop	Region	Sow	Harvest	$\bar{\theta}$	θ range
Maize	N America	May 02-Jun 01	Oct 15-Oct 31		
Maize	China	May 02-May 17	Sep 01-Sep 15		
Maize	Europe	Apr 01-May 01	Oct 01-Oct 31		
Maize	Global			0.80	0.72–0.88
Maize	Global			0.85*	0.72–0.93*
Spring Wheat	Canada	May 02-May 17	Sep 01-Sep 15		
Spring Wheat	NE China	Apr 01-Apr 16	Jul 16-Jul 31		
Spring Wheat	Central Asia	May 17-Jun 01	Jul 16-Jul 31		
Winter Wheat	United States	Sep 30-Oct 15	Jun 15-Jul 31		
Winter Wheat	Europe	Oct 15-Oct 30	Jun 15-Jul 31		
Winter Wheat	North China	Sep 15-Sep 30	Jun 01-Jun 16		
Wheat	Global			0.47	0.47–0.57
First Rice	China/C Asia	Apr 16-May 02	Sep 01-Sep 15		
Second Rice	China/S Asia	Jul 01-Jul 31	Nov 15-Nov 30		
Rice	Global			0.75	0.65–0.84
Soybeans	N America	Jun 01-Jun 16	Sep 30-Oct 15		
Soybeans	China	Apr 17-May 02	Sep 30-Oct 15		
Soybeans	Global			0.83	0.79–0.86
Soybeans	Global			0.85*	0.72–0.93*

Crop calendars from ref. 54 and the FluxNET-derived (denoted with an asterisk), and calendar-derived values for θ.